Photoinitiation Systems and Thermal Decomposition of Photodefinable Sacrificial Materials

Xiaoqun Wu,[1] Hollie A. Reed,[1] Larry F. Rhodes,[2] Ed Elce,[2] R. Ravikiran,[2] Robert A. Shick,[2] Clifford L. Henderson,[1] Sue Ann Bidstrup Allen,[1] Paul A. Kohl[1]

[1]*School of Chemical Engineering, Georgia Institute of Technology, Atlanta, Georgia 30332-0100*
[2]*Promerus LLC, 9921 Brecksville Road, Brecksville, Ohio 44141*

Received 5 March 2002; accepted 13 July 2002
Published online 18 February 2003 in Wiley InterScience (www.interscience.wiley.com). DOI 10.1002/app.11774

ABSTRACT: The exposure characteristics of norbornene-based photosensitive sacrificial materials as functions of the photoinitiator have been investigated. The results show that the initiator, bis(2,4,6-trimethylbenzoyl)-phenylphosphine oxide, provides high photosensitivity and an adjustable contrast factor. The kinetics of the thermal decomposition of the polymers have been investigated with dynamic and isothermal thermogravimetric analysis to determine the most appropriate conditions for the thermal decomposition of the sacrificial polymers. The reaction is slightly higher than first-order, and a single mechanism can account for the decomposition throughout the process. The dependence of the kinetic parameters on the composition of the copolymers has been studied, and the reaction order remains unchanged; however, the activation energy is lower when the alkenyl-substituted norbornene content is increased in the copolymers. © 2003 Wiley Periodicals, Inc. J Appl Polym Sci 88: 1186–1195, 2003

INTRODUCTION

Microfluidic devices have been extensively studied in recent years. They are being developed for numerous applications in medicine, biotechnology, analytical chemistry, and chemical synthesis.[1–5] The miniaturization of devices leads to many benefits, including low manufacturing costs, short analysis times, a low consumption of reagents and analytes, single-use devices, increased analysis accuracy, and high portability.[6,7] A common issue for the manufacturing of devices is the goal of a complex, three-dimensional (3D) network of interconnected microchannels enabling a wide variety of fluids to be selectively moved among microcomponents, such as micromixers, microvalves, micropumps, microreactors, and microseparators. The structure and fabrication method of the microchannels have an impact on the complexity and performance of the microfluidic devices.

The predominant commercial method for fabricating 3D microchannels is to bond together ultraflat glass plates with patterned channels.[8] There are disadvantages to this method, such as limitations in size and flatness, and the general difficulty of integrating electronic components into microfluidic devices.[8–10] A method has recently been proposed that uses conventional lithography and silicon fabrication technologies to make 3D microchannels that can be directly integrated with integrated circuit (IC) components.[11] This approach uses thermally decomposable polymers as placeholders that can be patterned into the image of the channels to be formed. Complex devices on silicon, glass, and other substrates can be formed by the sequential deposition of layers. After encapsulation, the polymer is thermally decomposed, and the products permeate through the overcoat material; this produces precisely defined channels. The formation of air channels with this processing technology for applications in compliant integrated circuit interconnection has been demonstrated.[12]

This approach avoids many of the problems with the glass-bonding method. However, it requires complex processing with many steps to pattern the sacrificial polymer materials. Also, it leaves unanswered the general need for 3D-shaped channels and components. As a solution to these problems, a simple and flexible method using direct patterning of the sacrificial material has been proposed (see Fig. 1).[13] This method significantly reduces the number of processing steps required to pattern the polymer features and makes it possible to produce channels with nonuniform heights with gray-scale lithographic masks.

The sacrificial material used in this method is formulated with a copolymer consisting of butylnorbornene and alkenyl-substituted norbornene (PNB) and a photoinitiator (PI).[14–16] As a sacrificial material, PNB has several advantages:

Correspondence to: P. A. Kohl (paul.kohl@che.gatech.edu).
Contract grant sponsor: National Science Foundation; contract grant number: DMI-9980804.

© 2003 Wiley Periodicals, Inc.

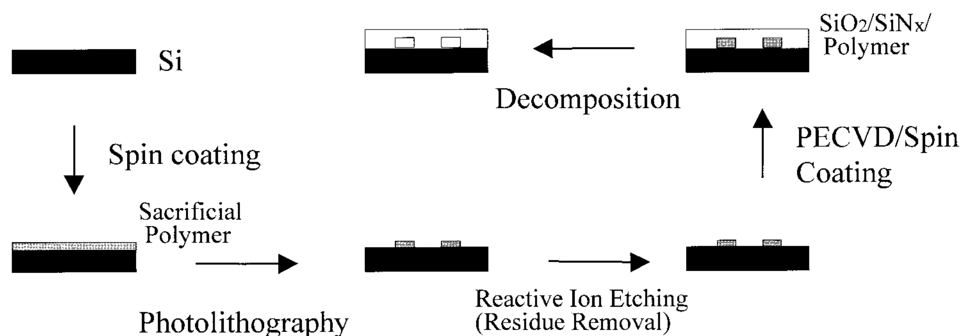

Figure 1 Scheme of the processing steps in the method using photopatternable sacrificial polymer materials.

1. PNB has a high glass-transition temperature that is about the same as its decomposition temperature (≥340°C).
2. PNB can undergo nearly complete decomposition that results in almost no residue.
3. The photodefinable properties of the polymer can be adjusted by changes in the nature and content of the functional side groups. As the formulated sacrificial material is exposed to ultraviolet (UV) light, the PI generates free radicals that initiate crosslinking reactions between double bonds in the alkenyl groups. The alkenyl content in the polymer and the PI loading strongly influence the exposure characteristics of the photosensitive system.[13]

TABLE I
Molecular Schemes of the PIs

PI	Molecular scheme
BEE	
Irgacure 907	
Irgacure 819	
Irgacure 651	
Irgacure 369	

However, the properties of the PI, including the UV absorption and efficiency of initiation of the crosslinking process, are also important factors in determining the characteristics of the photosensitive system. The goal of this study was to find an effective PI that could improve the sensitivity of the system.

The thermal decomposition of the encapsulated sacrificial polymer is the final step in the fabrication of the microchannels in this fabrication method. The conditions for the thermal decomposition need to be precisely set to prevent the channel structure from distorting during decomposition. A kinetic model of the thermal decomposition of the polymer is important because it can be used to select the conditions for optimum decomposition.

EXPERIMENTAL

Five PIs were selected for screening in the experiment: bis(2,4,6-trimethylbenzoyl)-phenylphosphine oxide (Irgacure 819, Ciba Specialty Chemicals, Inc., Basel, Switzerland), 2-benzyl-2-dimethylamino-1-(4-morpholinophenyl)-butanone-1 (Irgacure 369, Ciba Specialty Chemicals), 2,2-dimethoxy-1,2-diphenylethan-1-one (Irgacure 651, Ciba Specialty Chemicals), 2-methyl-1[4-(methyl-

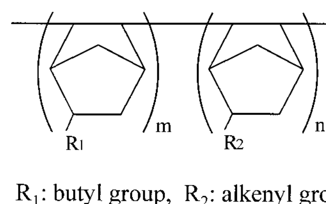

Figure 2 Generic structure of the polynorbornene copolymers.

TABLE II
Conditions and Results for UV Exposure Response Experiments with Different PIs and the Loading of Irgacure 819

Experiment	PI	Recipe of PNB/PI solution PNB1/PI/MS (wt %)	Photosensitivity (mJ/cm^2)	γ
1	BEE	16/0.64/83.36	1959	0.908
2	Irgacure 907	16/0.64/83.36	3641	0.651
3	Irgacure 651	16/0.64/83.36	1054	0.907
4	Irgacure 369	16/0.64/83.36	1808	0.521
5	Irgacure 819	16/0.64/83.36	134	1.213
6	Irgacure 819	16/0.32/83.68	363	0.879
7	Irgacure 819	16/0.16/83.84	3236	0.448

Processing conditions: spin-coating at 2400 rpm, softbake at 110°C for 1 min, PEB at 120°C, for 30 min, and developer-xylene.

thio)-phenyl]-2-morpholinopropan-1-one (Irgacure 907, Ciba Specialty Chemicals), and benzoin ethyl ether (BEE; Aldrich). The chemical formulas are given in Table I. The UV absorption characteristics of the PIs were studied with an HP 8453 ultraviolet–visible spectroscopy system. Methanol (>99.8%; Aldrich, Milwaukee, WI) was used to prepare PI solutions (0.012 wt % in methanol) for the UV absorption tests. In the tests, the PI solution was contained in a standard quartz cell (Fisher) with a path length of 10 mm. The thermal stability of the PIs was tested with a differential scanning calorimeter (DSC 220C, Seiko Instruments, Chiba, Japan). The differential scanning calorimetry (DSC) spectra were recorded at a heating rate of 3°C/min with a nitrogen purge rate of 28 mL/min.

The polynorbornene sacrificial polymers were synthesized with butyl norbornene (BuNB) and alkenyl norbornene (ANB) side groups by Promerus LLC (Brecksville, OH). The structure is shown in Figure 2. The molar ratio of butyl side groups to alkenyl side groups (BuNB/ANB) for most of the experiments was 77/23. Two reproductions of the polymer were used in this study. The weight-average molecular weight and polydispersity index for the two polymers were 276,100 and 4.22 for PNB1 and 241,400 and 4.1 for PNB2. In addition, a few experiments were performed at different BuNB/ANB ratios, which are described in the Results and Discussion section. Mesitylene (MS; 97%; Aldrich) was used as the solvent for the preparation of PNB/PI solutions, and xylene (>98.5%; Aldrich) was used to develop the exposed patterns.

The photosensitive PNB/PI solutions were prepared with the recipes listed in Table II and were stored in amber-glass bottles. Exposures were performed on silicon wafers (100 mm in diameter) spin-coated with the PNB/PI solutions and soft-baked. The thickness of the PNB/PI films was measured with a profilometer. An OAI mask aligner equipped with an *i*-line filtered UV irradiation source (365-nm wavelength) was used to expose the PNB/PI films. Before exposure, the intensity of the UV light source was measured with an OAI model 356 exposure analyzer with a 365-nm probe. The wafers were subjected to postexposure baking (PEB) with the same Brewer Science CEE 100 hot plate. After PEB, the samples were developed with a continuous spray of xylene while the wafer was spun at 500 rpm.

The decomposition characteristics of the polymers were investigated with a Seiko Instruments TG/DTA 320 system. The measurements were carried out in a nitrogen atmosphere at an N_2 purge rate of 28 mL/min.

Estimation of the kinetic parameters

Thermogravimetric analysis (TGA) measurements were obtained as weight losses as functions of the temperature or time [thermogravimetry (TG) curve] and as derivatives of weight losses as functions of the temperature or time [differential thermogravimetry (DTG) curve]. The fractional decomposition (α), as defined in eq. (1), can be calculated from the TG curves:

$$\alpha = \frac{W_0 - W}{W_0 - W_f} \tag{1}$$

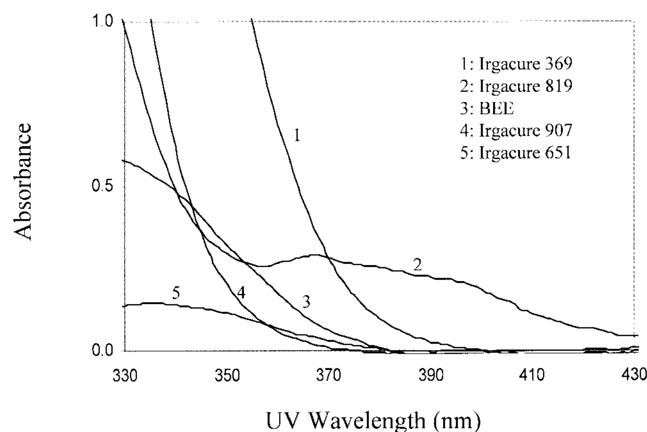

Figure 3 UV absorption curves for PI/methanol solutions with a concentration of 0.0012 wt %. The light path was 10 mm.

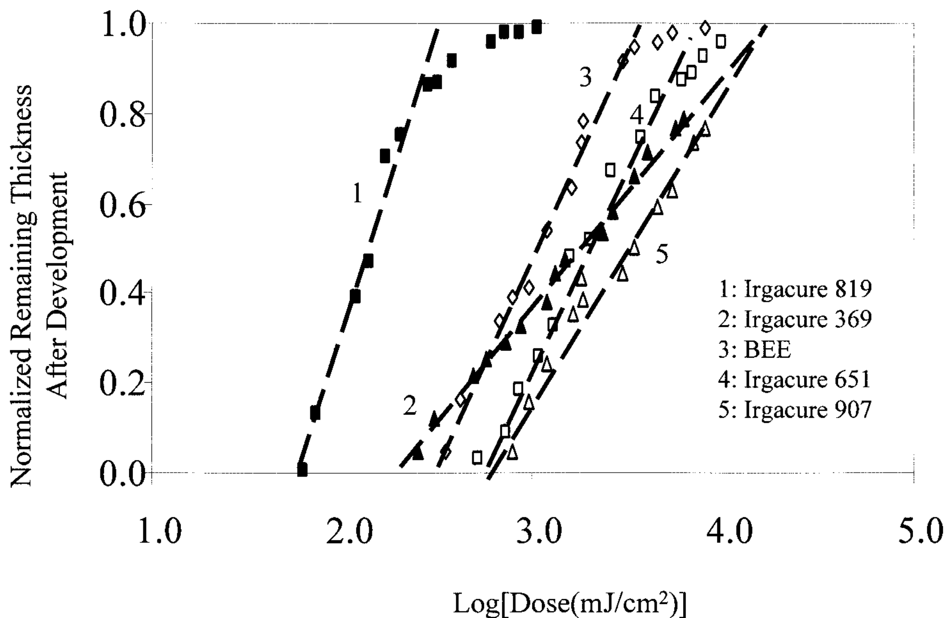

Figure 4 Contrast curves for photosensitive PNB formulations with various PIs at the same loading of 0.32 wt %.

where W_0 is the initial mass, W is the actual mass, and W_f is the final mass after decomposition. The kinetic mechanism of the thermal decomposition of the polymer is generally expressed as follows:

$$\frac{d\alpha}{dt} = k(1-\alpha)^n = A\exp\left(-\frac{E_\alpha}{RT}\right)(1-\alpha)^n \qquad (2)$$

where n is the order of the decomposition reaction, A is the Arrhenius pre-exponential factor, R is the gas constant, T is the temperature, k is the rate constant, and E_a is the activation energy. The decomposition rate ($d\alpha/dt$) can be calculated from the DTG curves. With a logarithmic transformation, eq. (2) becomes

$$\ln\left(\frac{d\alpha}{dt}\right) = \ln A - \frac{E_a}{RT} + n\ln(1-\alpha) \qquad (3)$$

The relationship of $\ln(d\alpha/dt)$ versus T^{-1} and $\ln(1-\alpha)$ is a linear function, and the kinetic parameters A, E_a, and n can be estimated by the fitting of this equation to the natural logarithmic derivative trend of mass loss with linear regression. This regression method requires both TG and DTG data for calculating $\ln(1-\alpha)$ and $\ln(d\alpha/dt)$ at different temperatures. The signal-to-noise ratio for the DTG curve is lower than that in the TG curve, and this could reduce the accuracy of the regression method with respect to the results obtained from the methods using only TG curves. The

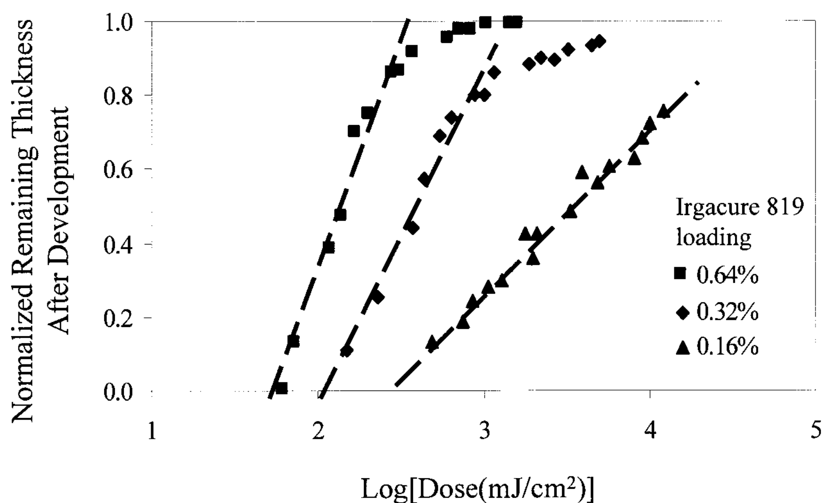

Figure 5 Contrast curves for photosensitive PNB formulations with various initiator (Irgacure 819) loadings.

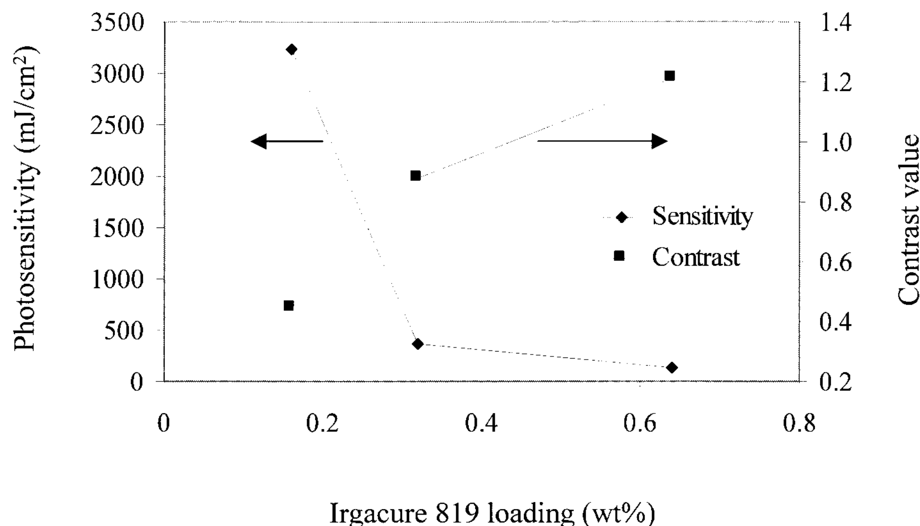

Figure 6 Sensitivity and contrast as functions of the loading of Irgacure 819.

accuracy of this method was discussed by Bockhorn et al.[17] Here, the data smoothing technique was applied to increase the signal-to-noise ratio of a measurement. A triangular weighted sliding average smoother was used in this work to preprocess the raw data before the regression manipulation:

$$S_i = \frac{\frac{m+1}{2} Y_i + \sum_{j=1}^{m-2} \frac{j+1}{2} [Y_{i-(m-j)/2} + Y_{i+(m-j)/2}]}{\frac{m+1}{2} + \sum_{j=1}^{m-2} (j+1)} \tag{4}$$

where S_i and Y_i are the smoothed signal and original signal for the ith point, respectively; $Y_{i\pm(m-j)/2}$ represents the original signals for the adjacent points of the ith point; j is equal to 1, 3, 5, …; and m is the smooth width if the odd number is taken, which is determined according to the purpose of the measurement and the sampling frequency.

For comparison, Ozawa's method,[18] which only uses dynamic TGA data with multiple heating rates, was used. This method shows the trend of E_a with temperature. Also, an isothermal method[19] manipulating isothermal TGA data was also applied for the estimation of the kinetic parameters. The advantages and drawbacks of dynamic and isothermal methods have been discussed in the literature.[19,20]

RESULTS AND DISCUSSIONS

Screening PI

The UV absorption behavior of the PI solutions was measured, and the results are shown in Figure 3. For the solutions containing Irgacure 651, Irgacure 907, and BEE, the absorbance at 365 nm is weak. The solutions with Irgacure 369 and Irgacure 819 show a strong absorbance at 365 nm. There are a number of factors influencing the initiation efficiency, including the absorption coefficient, yield of the radical formation, oxygen and monomer quenching, and reactivity of the radicals generated.[21] For a photoresist system, the primary factors considered in screening PIs are the photosensitivity, contrast value, and stability in thermal processing. High contrast is usually desired so that sharp patterns (steep walls) can be obtained. However, for the purpose of patterning 3D features, low contrast is needed. Therefore, the estimation of the photosensitivity and contrast was performed by the measurement of the normalized film thickness remaining after development as a function of the logarithmic exposure dose. The contrast data for 3.5–4.0-μm-thick (spin speed = 2100 rpm) PNB/PI films were

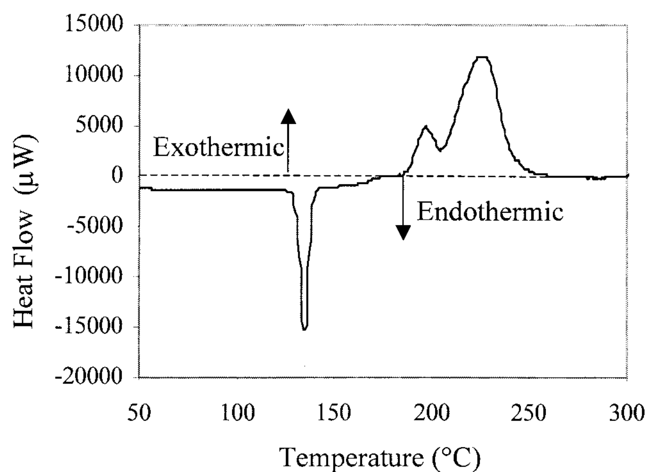

Figure 7 DSC spectrum of Irgacure 819.

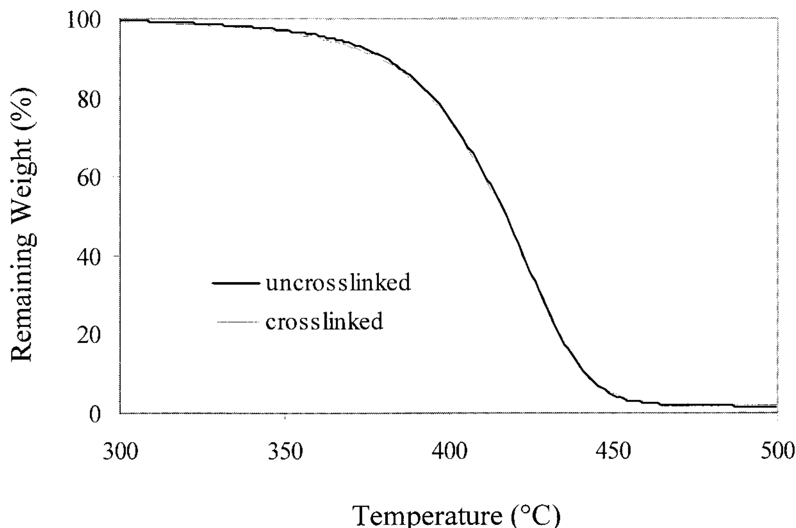

Figure 8 Dynamic TGA curves for crosslinked polymer and fresh polymer (PNB2) at a heating rate of 3.1°C/min.

measured after soft-baking at 110°C for 60 s and exposure to UV light. The films were postbaked at 120°C for 30 min, and the thicknesses of the films were measured after PEB and spray development with xylene. The contrast curves shown in Figure 4 were used to estimate the sensitivity and the dose required to achieve 50% original thickness after development. The contrast factor (γ) is evaluated with eq. (5):

$$\gamma = \frac{1}{\log\left(\frac{D^0}{D^i}\right)} \quad (5)$$

where D^i is the dose needed to produce full thickness after development and D^0 is the dose at the onset of the film remaining after development. From the curves in Figure 4, the sensitivity and γ values were estimated, and they are given in Table II. The sensitivities for the formulations containing Irgacure 651, Irgacure 907, and BEE are low. This result is consistent with the UV absorption of these initiators seen in Figure 3. However, the sensitivity for Irgacure 369 is also low, despite the high absorbance. Decker and Moussa[22] found that the yield of the radical formation

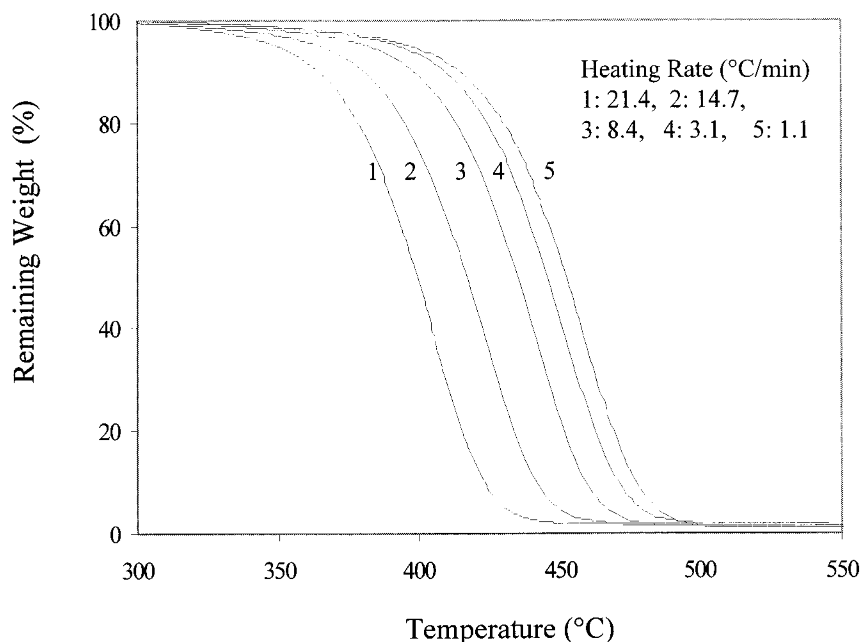

Figure 9 Dynamic TGA curves for PNB2 at different heating rates.

TABLE III
Kinetic Parameters for the Thermal Decomposition of PNB2 Obtained from Dynamic and Isothermal TGA Measurements

Method	Order of reaction	Pre-exponential factor (min^{-1})	E_a (kJ/mol)
Regression (dynamic)	1.08	1.96×10^{15}	214.2
Ozawa (dynamic)	1.12	2.32×10^{15}	214.8
Isothermal	1.22	7.30×10^{14}	208.0
Average	1.14	1.67×10^{15}	212.0

for Irgacure 369 was lower than for other initiators. In contrast, the sensitivity for Irgacure 819 is much higher than for the other systems. The high sensitivity for Irgacure 819 is due not only to a strong absorption at 365 nm but also to high radical initiation efficiency. Acylphosphine oxides have extensively been studied in recent years.[23–26] They have shown sufficient radical formation and high reactivity of the phosphinyl radicals.

The effect of the Irgacure 819 loading on the exposure characteristics of the photosensitive systems has been investigated. Three experiments with Irgacure 819 loadings of 0.16–0.64 wt % were performed (see Table II). The contrast curves for these samples are shown in Figure 5. The photosensitivity of the Irgacure 819 system is a strong function of its concentration in the solution. Figure 6 shows the sensitivity and contrast versus the loading for Irgacure 819 calculated from Figure 5. An increase in the Irgacure 819 concentration increases the photosensitivity and contrast value. For the 0.32 wt % loading, the sensitivity is much higher than that for the other PI systems with a 0.64 wt % loading, and a contrast value lower than some of the others is maintained. This high sensitivity and low contrast for Irgacure 819 are desirable for the patterning of 3D features. In common photoresist applications, high sensitivity and high contrast are desirable for creating sharp, two-dimensional features with nearly vertical side walls.

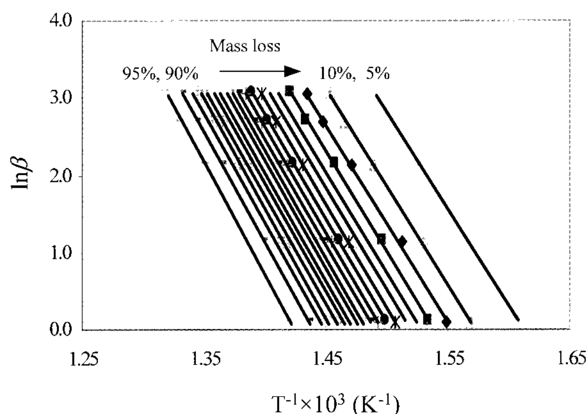

Figure 10 Plot of ln β versus T^{-1} based on Ozawa's method.

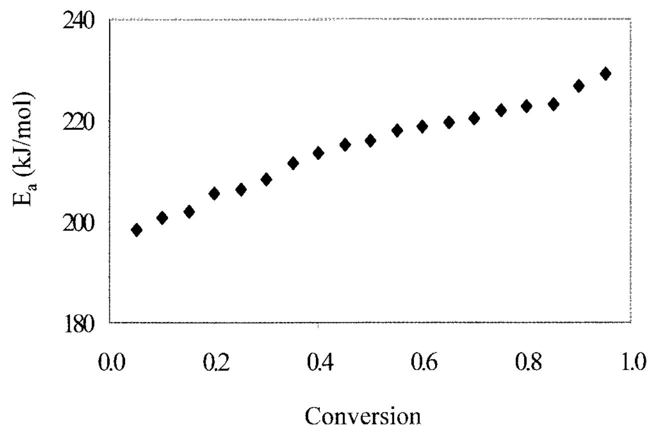

Figure 11 Plot of E_a versus the decomposition conversion for PNB2.

The thermal stability of Irgacure 819 PIs has been investigated with DSC, as shown in Figure 7. The endothermic peak (downward direction) at 140°C corresponds to the melting transition. Two exothermic peaks are the result of reactions occurring between the reactive species generated from decomposed Irgacure 819. The initial temperature of the thermal decomposition for Irgacure 819 is 168°C (the initial temperature of the first exothermic peak). Therefore, its thermal stability is compatible with the thermal processing steps used in soft baking and PEB.

Thermal decomposition

A crosslinked polymer sample was prepared with the following process steps. First, a film was made by the spin coating of a polymer solution (PNB2/Irgacure819/MS = 16/0.32/83.68) onto an oxidized silicon wafer at a speed of 2400 rpm and by soft baking at 110°C for 60 s. Next, the film was exposed to UV light at a dose of 6000 mJ/cm^2, and this was followed by postbaking at 120°C for 40 min. The film was spray-developed with xylene, and then the film was peeled off the wafer through soaking in a 49 wt % HF solution. Finally, the film was rinsed with deionized water and dried in an oven at 120°C for 1 h. A TGA analysis was performed at a heating rate of 3.1°C/min. The TGA analyses of the exposed (crosslinked) and uncrosslinked film are shown in Figure 8. There is no significant difference in the thermal stabilities of the two films. This implies that the thermal decomposition of the crosslinked polymer is dominated by polynorbornene main-chain scission, as in the uncrosslinked polymer. Therefore, it is equally valuable to study the kinetics of the uncrosslinked polymer.

A series of TG measurements were performed at heating rates of 1.1, 3.1, 8.4, 14.7, and 21.4°C/min to

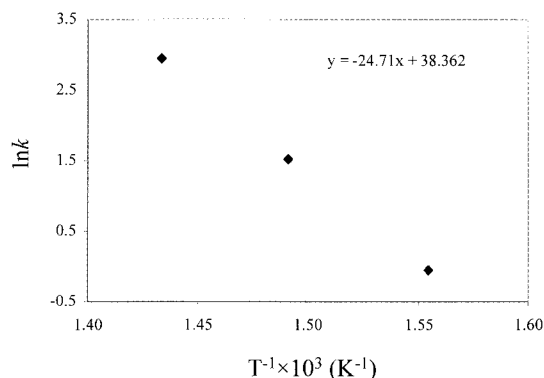

Figure 12 Plot of the Arrhenius relationship, ln k versus T^{-1}, for the isothermal TGA measurements.

study the kinetics of PNB2. The dynamic TGA curves under nitrogen for PNB2 are shown in Figure 9. The TGA curves indicate that the polymer can be completely pyrolyzed in a nitrogen atmosphere. Only a single step in the thermal degradation can be seen. The results show a strong dependence of the thermal degradation behavior of the polymer on the heating rate.

To reduce the noise in the DTG data, seven-point smoothing was used to preprocess the raw data. The regression of the smoothed DTG data gave an estimate of the kinetic parameters for the heating rates. When α approaches 0 or 1, $d\alpha/dt$ approaches zero, and so the numerical error is high. Therefore, only the mass changes in the range of 1–99% have been used.[17] The average kinetic parameters from the regression are shown in Table III.

Ozawa's method has often been used to manipulate the dynamic TGA measurements in the literature because it can show the changes in E_a versus conversion in the decomposition process.[18] With Ozawa's method used to study the TGA data shown in Figure 9, a plot of ln β versus T^{-1} at different degrees of conversion was obtained (Fig. 10) to give a series of straight lines where β is the dimensionless Ozawa parameter. From the slope of the lines, E_a as a function of conversion was estimated. Figure 11 shows that E_a increases slightly from 199 to 229 kJ/mol for 5–95% weight losses.

In the dynamic measurements, the temperature difference within the sample and outside the sample could be a source of error for rapid heating rates. This drawback can be avoided with an isothermal measurement. Therefore, the isothermal method has also been used to calculate kinetic parameters. Isothermal TGA measurements for 370.7, 397.5, and 424.5°C were performed with a nitrogen purge rate of 28 mL/min. The reaction order and rate constant of degradation at various temperatures were calculated. The preexponential factor and E_a were obtained from the Arrhenius plot in Figure 12. The average values of the kinetic parameters calculated from the three methods are summarized in Table III. The results are within experimental error in the measurements. The order of thermal decomposition is slightly higher than one.

Because of its simplicity, the multiple regression method was used to estimate the kinetic parameters of thermal decomposition for the polymers. The TGA measurements for PNB1, PNB2, PNB3, and PNB4, were performed at a heating rate of 3°C/min and at a nitrogen purge rate of 28 mL/min. The TGA curves are shown in Figure 13. The temperatures $T_{5\%}$, $T_{50\%}$, $T_{95\%}$, and $T_{\max}$ and the residue at 550°C are given in Table IV. The results show that $T_{5\%}$ shifts to low values (371–363°C) as the ANB content increases from 10 to 50 mol %, and this reflects the initial decomposition temperature becoming lower. However, $T_{95\%}$

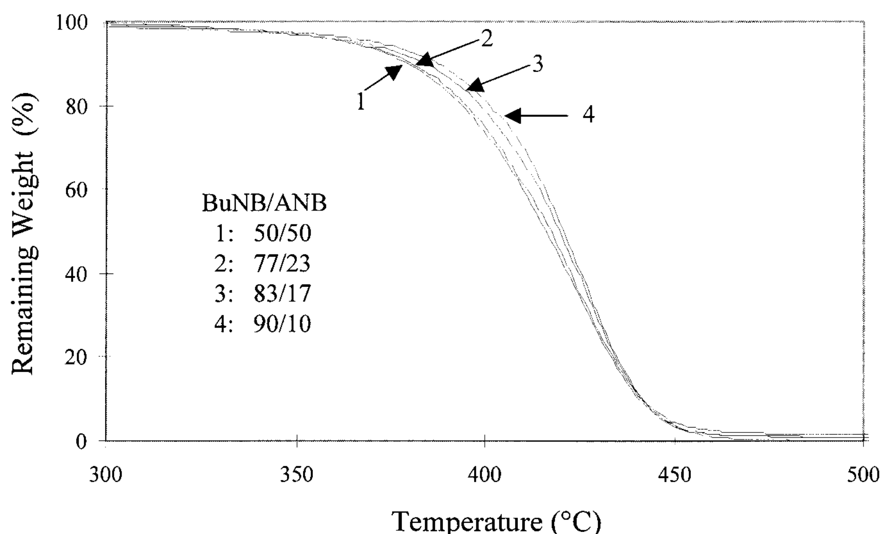

Figure 13 Dynamic TGA curves for various ANB contents of PNB at a heating rate of 3.1°C/min.

TABLE IV
Characteristic Temperatures and Residues for the Thermal Decomposition of PNB with Varying ANB Content at Heating Rate of 3.1°C/min

BuNB/ANB of PNB	$T_{5\%}$ (°C)	$T_{95\%}$ (°C)	$T_{50\%}$ (°C)	Residue at 550°C (%)
90/10	363	447	416	0.9
83/17	364	448	417	0.8
77/23	366	449	420	1.6
50/50	371	447	421	0.0

varies slightly, within a range of 2°C, as the ANB content changes. As a result, the substitution of ANB mainly affects the thermal degradation behavior of the polymer during the initial stage. The thermal degradation of polymers is usually characterized by the breaking of the weakest bond and so is determined by this bond dissociation energy.[27] It may be expected that the temperature at which the same amount of degradation is reached is basically proportional to the particular bond dissociation energy. The weakest bond involved in the alkenyl group is about 230 kJ/mol. With an increase in the number of alkenyl groups substituted for butyl groups, a shift of TGA curves to lower temperature ranges (especially for the initial stage of decomposition) can be expected.

The changes in E_a and the reaction order versus the ANB content are plotted in Figure 14. It illustrates that the reaction order is nearly independent of the ANB content. E_a decreases as the ANB content increases, and this agrees with the previous discussion on the bond dissociation. Wedlake,[28] in his investigation into the decomposition of the homopolymer of BuNB, used Ozawa's method to approach the dynamic TGA measurements with different heating rates. He established that a first-order reaction occurs with an average E_a value of 228.3 kJ/mol. According to the trend of E_a plotted in Figure 14, this value (228.3 kJ/mol for the homopolymer of BuNB) is slightly low but still falls in the trend range.

CONCLUSIONS

Two important aspects of photosensitive sacrificial materials have been investigated: the photoinitiation efficiency and the kinetics of thermal decomposition. Various PIs have been screened, and the study indicates that the initiator bis(2,4,6-trimethylbenzoyl)-phenylphosphine oxide (Irgacure 819, Ciba Specialty Chemicals) exhibits an impressive performance, showing high photosensitivity, an adjustable γ value for the photosensitive system, and good thermal stability. These features are desirable in a photosensitive system for fabricating microchannels with a gray-scale cross-section shape.

The kinetics of the thermal decomposition of the sacrificial polymers has been studied with dynamic and isothermal TGA experiments. Kinetic parameters were calculated by the application of the multiple regression technique, Ozawa's method, and isothermal treatment. The obtained results agree with one another and also indicate that the reaction order is a little higher than one and that the mechanism of the reaction remains nearly consistent during the whole decomposition process. The multiple regression method, combined with data smoothing, is an effective and simple method for calculating the kinetic parameters based on the dynamic TGA measurements. It has been employed to investigate the relationship of the kinetics of thermal decomposition changing with the ANB content in PNB. The results demonstrate that the reaction order remains un-

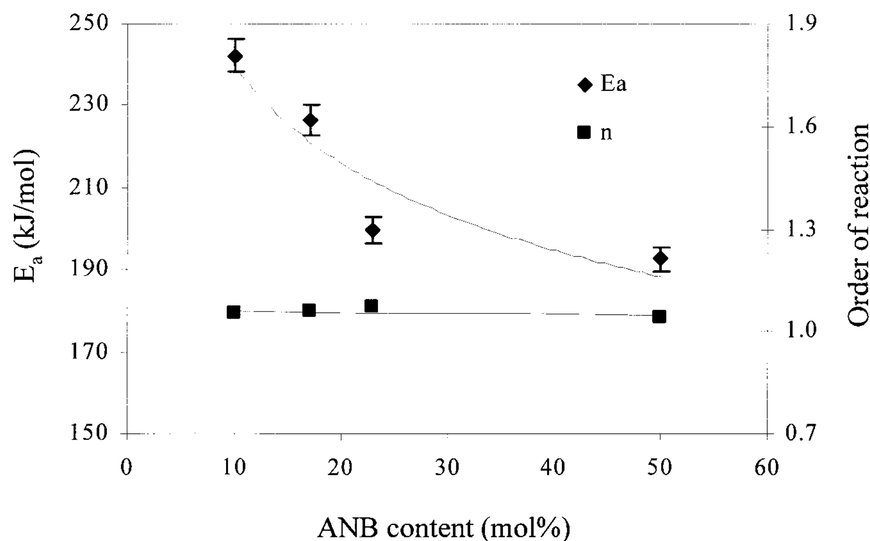

Figure 14 E_a and the reaction order of the thermal decomposition as functions of the ANB content of PNB.

changed and that E_a decreases as the ANB content in PNB increases.

References

1. Gravensen, P.; Branebjerg, J.; Jensen, O. S. J Micromech Microeng 1993, 3, 168.
2. Service, R. F. Science 1998, 282, 396.
3. Mastrangelo, C. H.; Burns, M. A.; Burke, D. T. Proc IEEE 1998, 86, 1769.
4. Moukheiber, Z. Forbes 1998, 161, 76.
5. Srinivasan, R.; Hsing, I.-M.; Ryley, J.; Harold, M. P.; Jensen, K. F.; Schmidt, M. A. Proc Solid State Sens Actuator Workshop 1996, p 15.
6. McDonald, J. C.; Duffy, D. C.; Anderson, J. R.; Chiu, D. T.; Wu, H.; Schueller, O. J. A.; Whitesides, G. M. Electrophoresis 2000, 21, 27.
7. Nguyan, N.-T.; Weveley, S. Fundamentals and Applications of Microfluidics and Microelectromechanical Systems; Artech House: New York, 2002.
8. Raley, N. F.; Davidson, J. C.; Balch, J. W. Proc SPIE 1997, 3224, 185.
9. Raley, N. F.; Davidson, J. C.; Balch, J. W. Proc SPIE 1998, 2639, 40.
10. Pethig, P.; Burt, J. P. H.; Parton, A.; Rizvi, N.; Talary, M. S.; Tame, J. A. J Micromech Microeng 1998, 8, 356.
11. Bhusari, D.; Reed, H.; Wedlake, M.; Padovani, A.; Bidstrup Allen, S. A.; Kohl, P. IEEE J Microelectromech Syst 2001, 10, 400.
12. Meindl, J. D.; Davis, J. A.; Zarkesh-Ha, P.; Patel, C.; Martin, K.; Kohl, P. A. IBM Res J 2002, 46, 245.
13. Wu, X. Q.; Reed, H. A.; Rhodes, L. F.; Elce, E.; Ravikiran, R.; Shick, R. A.; Henderson, C. L.; Bidstrup Allen, S. A.; Kohl, P. A. J Electrochem Soc 2002, 149, 6555.
14. Rhodes, L. F.; Goodall, B. L.; Mulhaupt, R.; Shick, R. A.; Benedikt, G. M.; Jayaraman, S. K.; Soby, L. M.; McIntosh, L. H. U.S. Patent 6,294,616 (2001).
15. Goodall, B. L.; Risse, W.; Mathew, J. P. U.S. Patent 5,705,503 (1998).
16. Goodall, B. L.; Benedikt, G. M.; McInstosh, L. H.; Barnes, D. A. U.S. Patent 5,468,819 (1995).
17. Bockhorn, H.; Hornung, A.; Hornung, U.; Teepe, S.; Weichmann, J. Combust Sci Technol 1996, 116, 129.
18. Ozawa, T. Bull Chem Soc Jpn 1965, 38, 1881
19. Goodall, C. In Modern Methods of Data Analysis; Fox, J.; Long, J. S., Eds.; Sage: Beverly Hills, CA, 1990; Chapter 3.
20. Bockhorn, H.; Hornung, A.; Hornung, U. J Anal Appl Pyrolysis 1999, 50, 77.
21. Fouassier, J. P. In Radiation Curing in Polymer Science and Technology; Fouassier, J. P.; Rabek, J. F., Eds.; Elsevier Science: New York, 1993; Vol. 1, p 49.
22. Decker, C.; Moussa, K. Makromol Chem 1990, 191, 963.
23. Baxter, J. E.; Davidson, R. S. Makromol Chem 1988, 189, 2769.
24. Decker, C. Prog Polym Sci 1996, 21, 593.
25. Rutsch, W.; Dietliker, K.; Leppard, D.; Kohler, M.; Misev, L.; Kolczak, U.; Rist, G. Prog Org Coat 1996, 27, 227.
26. Decker, C.; Zahouily, K.; Decker, D.; Nguyen, T.; Eiet, T. Polymer 2001, 42, 7551.
27. Van Krevelen, D. W. Properties of Polymers, 3rd ed.; Elsevier Science: New York, 1990; Chapter 21.
28. Wedlake, M. D. Master's Thesis, Georgia Institute of Technology, 2000.